

On Approximating Discontinuous Solutions of PDEs by Adaptive Finite Elements

Shun Zhang

Department of Mathematics, City University of Hong Kong, Hong Kong SAR, China

Keywords: discontinuous solution of PDE, overshooting, adaptive finite element methods, singularly perturbed equation, Gibbs phenomena

Abstract. For singularly perturbed problems with a small diffusion, when the transient layer is very sharp and the computational mesh is relatively coarse, the solution can be viewed as discontinuous. For both linear and nonlinear hyperbolic partial differential equations, the solution can be discontinuous. When finite element methods with piecewise polynomials are used to approximate these discontinuous solutions, numerical solutions often overshoot near a discontinuity. Can this be resolved by adaptive mesh refinements?

In this paper, for a simple discontinuous function, we explicitly compute its continuous and discontinuous piecewise constant or linear projections on discontinuity matched or non-matched meshes. For the simple discontinuity-aligned mesh case, piecewise discontinuous approximations are always good. For the general non-matched case, we explain that the piecewise discontinuous constant approximation combined with adaptive mesh refinements is the best choice to achieve accuracy without overshooting. For discontinuous piecewise linear approximations, non-trivial overshootings will be observed unless the mesh is matched with discontinuity. For continuous piecewise linear approximations, the computation is based on a "far away assumption", and non-trivial overshootings will always be observed under regular meshes. We calculate the explicit overshooting values for several typical cases.

Email address: shun.zhang@cityu.edu.hk (Shun Zhang)

¹This work was supported in part by Hong Kong Research Grants Council under the GRF Grant Project No. 11305319, CityU.

Several numerical tests are performed for a singularly-perturbed reaction-diffusion equation and linear hyperbolic equations to verify our findings in the paper.

1. Introduction

For a wide range of partial differential equations, their solutions can be discontinuous. For example, for singularly perturbed problems, when the transient layer is very sharp, the solution can be viewed as discontinuous, see [12, 4]. For linear and nonlinear hyperbolic equations, the discontinuous solutions can be caused by a discontinuous initial data or shock forming, see [7, 6]. Sometime, the location of discontinuity is known, for example, the discontinuity in the initial or boundary data. For many other cases, the exact location of discontinuity is unknown. When different numerical methods are used to solve such problems, the numerical solutions are often *oscillatory* near a discontinuity, i.e., it overshoots (and undershoots). In spectral methods and Fourier analysis, it is also called the Gibbs phenomena, see [8, 5]. Such spurious oscillations are unacceptable for many situations, see for example, page 209 of Hesthaven [6]. Such oscillations are essentially caused by a simple fact: continuous functions are used to approximate a discontinuous function. In numerical methods, some tricks are used to eliminate or reduce the Gibbs phenomena: artificial viscosity, limiters, filters, and ENO/WENO schemes, see [7, 6, 5].

On the other hand, it is well known that adaptive finite element method with mesh refinements based on a posteriori error estimation is a very useful procedure to detect the regions and locations with bad approximations, see [15]. A common adaptive finite element algorithm contains the loops of the following steps:

SOLVE \longrightarrow ESTIMATE \longrightarrow MARK \longrightarrow REFINE/COARSEN

The SOLVE step solves the numerical problems. The ESTIMATE step computes the a posteriori error estimates and indicators. The MARK step marks these elements with big error indicators or small error indicators. The REFINE step refines those elements marked with big error indicators. For some advanced algorithms, an extra COARSEN step is applied to combine these elements with small error indicators. If the solution is discontinuous and often badly approximated, an accurate a posteriori error estimator can often mark these badly approximated elements..

But can *adaptive finite element methods get accurate approximations of discontinuous solutions of PDEs without overshooting?* For this question, there are some confusing and conflicting folklores: 1. an adaptive mesh cannot reduce the overshootings. This is the common opinion in the numerical hyperbolic equations community with finite difference/finite volume methods, see [1, 13]. 2. When the mesh is fine enough, the discontinuity is resolved, the overshooting can be reduced. This opinion is probably more common in the adaptive finite element method community where *the adaptivity can almost cure everything* is believed. 3. Since the solution is discontinuous, if methods based on discontinuous piecewise polynomials, for example, discontinuous Galerkin (DG) methods, are used, the overshootings can be eliminated or reduced. For example, in a numerical computation for a singularly perturbed problem in a SIAM review paper [4] (p. 165), the authors claimed the DG methods will have no overshootings for almost discontinuous solutions.

In this paper, we want to clarify this question by a simple model problem. Since most of the finite element or DG methods are based on projections or pseudo-projections, the best result a numerical method can achieve of a certain approximation often cannot be better than its L^2 -projection, i.e., if V_h is the discrete approximation space, the best we can hope for the numerical error is often in the form (many methods cannot have such a good result, for example, the DG method for the linear hyperbolic equation):

$$\|u - u_h\|_0 \leq C \inf_{v_h \in V_h} \|u - v_h\|_0 = C \|u - \Pi_{V_h} u\|_0,$$

where Π_{V_h} is the L^2 projection operator onto the discrete approximation space V_h . For a step function u , we try to study the properties of $\Pi_{V_h} u$ under a refined mesh to answer the above question.

Based on the computations, we find the following results. For the simple discontinuity-aligned mesh case, piecewise discontinuous approximations are always good. For the general non-matched case, we explain that **the piecewise discontinuous constant approximation combined with adaptive mesh refinements is the best choice to achieve accuracy without overshooting**. For discontinuous piecewise linear approximations, non-trivial overshootings will be observed unless the mesh is matched with discontinuity. For continuous piecewise linear approximations, non-trivial overshootings will always be observed under regular meshes. We calculate the explicit overshooting values for several typical cases.

We also find that a special high ratio mesh obtained by adaptive mesh refinements combined with coarsening can also reduce the overshooting. But such case is not always possible in two and three dimensions or in one dimension with other error sources.

The paper is organized as follows. Section 2 describes a model problem of approximating a step function by L^2 projections onto piecewise constant and linear function spaces. Discontinuous piecewise constant and linear approximations are explicitly computed for the model problem in Section 3. In Section 4, we compute continuous piecewise linear approximations for the model problem under a "far away assumption". In Section 5, linear conforming, linear DG, and lowest order mixed finite element methods are tested on a one dimensional singularly perturbed problem. Several test problems of 2D linear transport problems with P0- and P1-DGFEMs are done in Sections 6. In Section 7, we make some concluding remarks.

2. A Model Problem

Consider a step function u :

$$u(x) = \begin{cases} -1 & x < 0, \\ 1 & x > 0. \end{cases} \quad (2.1)$$

Here, the discontinuity gap $u(0+) - u(0-)$ is 2. For more general cases with a gap $2c$, $c > 0$, it is easy to see the corresponding results are also proportional to c .

Let $\mathcal{T}_h = \{K\}$ be a one-dimensional mesh on $\Omega = (-a, b)$ with elements (intervals in the 1D setting) denoted by K . We suppose a and b are big enough positive numbers with respect to the mesh size. Let $P_k(K)$ be the space with polynomials defined on K whose degree is less or equal to integer $k \geq 0$. We consider three approximation spaces defined on \mathcal{T}_h :

$$P_0(\mathcal{T}_h) := \{v \in L^2(\Omega) : v|_K = P_0(K), \forall K \in \mathcal{T}_h\}, \quad (2.2)$$

$$P_1(\mathcal{T}_h) := \{v \in L^2(\Omega) : v|_K = P_1(K), \forall K \in \mathcal{T}_h\}, \quad (2.3)$$

$$S_1(\mathcal{T}_h) := \{v \in C^0(\Omega) : v|_K = P_1(K), \forall K \in \mathcal{T}_h\}. \quad (2.4)$$

Let X_h be $P_0(\mathcal{T}_h)$, $P_1(\mathcal{T}_h)$, or $S_1(\mathcal{T}_h)$, the L^2 projection $u_h \in X_h$ is defined by:

$$(u_h, v_h)_\Omega = (u, v_h)_\Omega \quad \forall v_h \in X_h.$$

We use notations $u_{h,0}$, $u_{h,1}$, and $u_{c,1}$ to denote the L^2 -projections of u on $P_0(\mathcal{T}_h)$, $P_1(\mathcal{T}_h)$, and $S_1(\mathcal{T}_h)$, respectively.

3. Discontinuous Approximations

In this section, we consider two discontinuous approximations: P_0 and P_1 approximations. Note that, for a discontinuous projection, the approximation is exact on those elements which are away from the discontinuity. Thus, we only need to discuss the special interval that contains the discontinuity.

Let $0 \leq t \leq 1$ and $h > 0$, we will consider the interval $I_0 = (-th, (1-t)h)$, see (a) of Fig. 1.

3.1. Discontinuous piecewise constant approximation

A simple computation shows that the constant projection of u on the interval I_0 is:

$$u_{h,0}|_{I_0} = 1 - 2t. \quad (3.1)$$

It is obvious that $-1 \leq 1 - 2t \leq 1$ for $t \in [0, 1]$, thus there is **no overshooting**. If $t = 0$ or 1 , which corresponds to the cases that the discontinuity is matched with the mesh, the numerical approximation is exact.

Compute the L^2 error in the interval I_0 , we have,

$$\|u - u_{h,0}\|_{0,I_0} = 2\sqrt{t(1-t)h}. \quad (3.2)$$

The worst case is $\|u - u_{h,0}\|_{0,I_0} = \sqrt{h}$, when $t = 1/2$. This also matches the a priori analysis that $\|u - u_{h,0}\|_{0,I_0} \leq Ch^{1/2-\epsilon}$ for $u \in H^{1/2-\epsilon}(I_0)$ for an arbitrary small $\epsilon > 0$.

With a good a posteriori error estimator that can identify the bad approximated elements, the discontinuity-crossing elements will be found and divided. The L^2 and other integration based norms of error will become smaller and smaller. Thus, for this case, the adaptive finite element methods do can achieve accuracy without overshooting.

3.2. Discontinuous piecewise linear approximation

In this subsection, we consider the L^2 projection of u onto a linear function on I_0 . To this end, let λ_{-1} and λ_1 be the linear Lagrange basis functions define on $(-th, (1-t)h)$ with $\lambda_i(z_i) = 1$, $\lambda_i(z_{-i}) = 0$, where $i = 1$ or -1 , and $z_{-1} = -th$ and $z_1 = (1-t)h$.

Let the projection $u_{h,1}|_{I_0} = U_{-1}\lambda_{-1} + U_1\lambda_1$. The projection problem is then

$$\begin{pmatrix} (\lambda_{-1}, \lambda_{-1})_{I_0} & (\lambda_1, \lambda_{-1})_{I_0} \\ (\lambda_{-1}, \lambda_1)_{I_0} & (\lambda_1, \lambda_1)_{I_0} \end{pmatrix} \begin{pmatrix} U_{-1} \\ U_1 \end{pmatrix} = \begin{pmatrix} (u, \lambda_{-1})_{I_0} \\ (u, \lambda_1)_{I_0} \end{pmatrix}.$$

Note that all terms of the matrix problem can be computed exactly. Solve the projection problem, we get

$$U_{-1} = 1 - 8t + 6t^2 \quad \text{and} \quad U_1 = 1 + 4t - 6t^2.$$

It is easy to show that

$$\begin{aligned} (U_1 - 1) > -(U_{-1} + 1) &\geq 0 && \text{if } 0 < t < 1/2, \\ -(U_{-1} + 1) > (U_1 - 1) &\geq 0 && \text{if } 1/2 < t < 1. \end{aligned}$$

The overshooting value can be defined as the following function:

$$\text{os} = \max(U_1 - 1, -(U_{-1} + 1), 0).$$

We plot the value of os for $0 \leq t \leq 1$ on the right of Fig. 1. It is easy to see that only when the mesh is aligned with the discontinuity ($t = 0$ or 1), os is zero. For t away from 0 or 1, the overshooting phenomena is severe. The maximum overshooting value $2/3$ appears at $t = 1/3$ or $2/3$.

We also notice that if the bisection is used, the relative position of the discontinuity normally will not converges to the left or the right point of the interval. For example, consider the the interval $(-1/3, 2/3)$, i.e., the discontinuity is at the $1/3$ position of the interval, if we bisect the interval, the new interval contains the discontinuity is $(-1/3, 1/6)$, the discontinuity is at the $2/3$ position. Keeping doing the bisection, we will find that the discontinuity will jump between the $1/3$ and $2/3$ positions. In this case, t will always be $1/3$ or $2/3$, the overshooting value will not decrease. For other initial positions other than the matched case, the overshooting values will oscillate between $[\delta, 2/3]$, for some $0 < \delta < 2/3$.

Compute the L^2 error in the interval I_0 , we have,

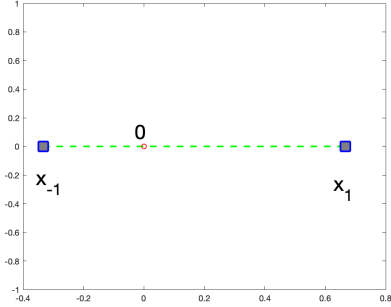
$$\|u - u_{h,1}\|_{0,I_0} = 2\sqrt{t(1-t)(1-3t+3t^2)}h.$$

When $t = 0$ or 1 , the error is zero. The largest error $\sqrt{h/3}$ appears at $t = 0.5 \pm \frac{1}{2\sqrt{3}}$.

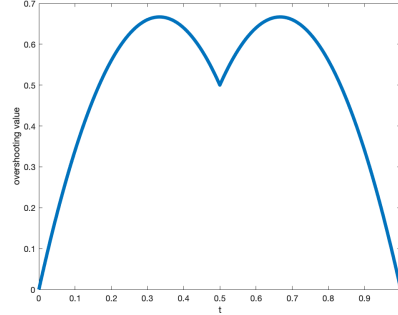
Note that $1/4 \leq 1 - 3t + 3t^2 \leq 1$ for $0 \leq t \leq 1$, thus we have

$$\|u - u_{h,1}\|_{0,I_0} \leq \|u - u_{h,0}\|_{0,I_0}.$$

Thus, for discontinuous approximations, even though that the L^2 -norm of error of the P_1 approximation is better than the P_0 approximation, they are of the same order if the mesh is not aligned, and the overshooting cannot be avoided in most cases.



(a) the interval I_0



(b) overshooting values as $t \in (0, 1)$

Figure 1: Discontinuous piecewise linear approximation on a discontinuity non-aligned mesh

4. Continuous Piecewise Linear Approximation

For the continuous piecewise linear approximation, the exact solution is not in the approximation space even for the discontinuity matched case, and the projection is not local to one element anymore. Luckily, based on the numerical experiments, we can safely assume the following **far away assumption** for the continuous piecewise linear approximation.

Assumption 4.1. Approximation on nodes far away from the discontinuity (far away assumption): For a node x_k of the mesh \mathcal{T}_h , if there is at least one node between the discontinuity position and x_k , the value of $u_{c,1} \in S_1$ at x_k is very close to the exact value of u .

4.1. Discontinuity matched mesh

We first consider a possible ideal case: the mesh is aligned with the discontinuity and the mesh is symmetric with respect to the discontinuity at 0.

Let \mathcal{T}_h be a symmetric mesh on $[-1, 1]$ with nodes: $x_{-N} < x_{-N+1} < \dots < x_{-1} < x_0 < x_1 < \dots < x_{N-1} < x_N$, where $x_{-i} = -x_i$ and $x_0 = 0$.

We first test on a uniform mesh with $h = 1/N$ and $x_{\pm i} = \pm ih$. We observe a consistent pattern is observed for different h .

From the numerical tests, for example, $h = 1/16$ and $h = 2^{-14}$ in Fig. 2, we note that the values of $u_{c,1}$ at the center nodes $x_{\pm i}$ are identical for different choice h for $i \leq 4$. For i big enough, $u_{c,1}(x_{\pm i})$ is almost identical to u .

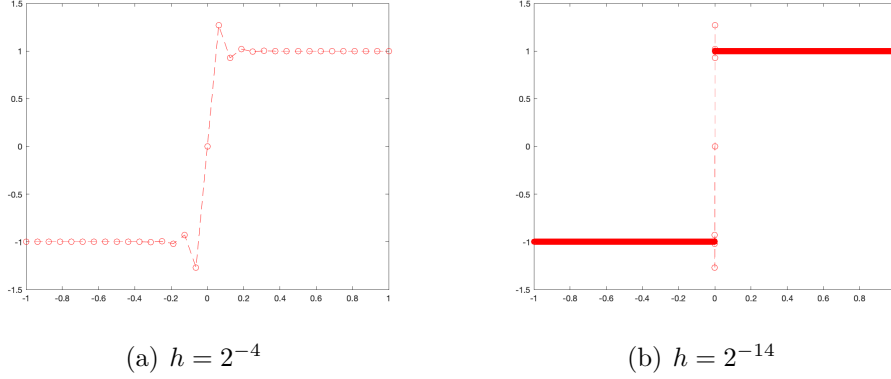


Figure 2: Continuous piecewise linear approximations on a uniformly refined mesh

The values $u_{c,1}(x_i)$ for $i = -4, -3, \dots, 3, 4$ are $-0.9948, -1.0192, -0.9282, -1.2679, 0, 1.2679, 0.9282, 1.0192,$ and 0.9948 . The severe overshootings only appear on the two nodes around the discontinuity. The far away assumption is clearly true in this case.

With the far away assumption, a simple calculation can be done to show why the values of $u_{c,1}$ at $x_{\pm 1}$ are close to ± 1.25 . We simplify the calculation by assuming that $u_{c,1} = u$ at all $x_{\pm i}, i > 2$. We assume the values of $u_{c,1}(x_{\pm 2}) = \pm(1 + \epsilon)$, where $|\epsilon|$ is a small number compared to 1. We have the rest three values at $x_{\pm 1}$ and x_0 to be computed by the projection. By the symmetry of nodes, it is easy to see that $u_{c,1}$ at $x_0 = 0$ is 0 and $u_{c,1}(x_i) = -u_{c,1}(x_{-i})$. Thus we only need to determine the value of $u_{c,1}(x_1) =: U_1$. Let λ_1 and λ_2 be the linear Lagrange basis functions on the mesh, with $\lambda_i(x_j) = \delta_{i,j}, i, j \in \{1, 2\}$. Then $u_{c,1}$ on (x_0, x_2) can be written as

$$u_{c,1} = U_1 \lambda_1 + (1 + \epsilon) \lambda_2, \quad x \in (x_0, x_2),$$

The value of U_1 can be obtained by a simple projection:

$$(U_1 \lambda_1 + (1 + \epsilon) \lambda_2, \lambda_1)_{(x_0, x_2)} = (1, \lambda_1)_{(x_0, x_2)}.$$

A simple calculation shows

$$U_1 = 1.25 - \epsilon/4.$$

Thus, the overshooting value is always close to $1/8$ of the discontinuity jump (2 in our example). The exact value 1.2679 is due to the fact ϵ is about -0.0718 in the example.

The L^2 errors in the two adjacent elements of 0 is also easy to compute,

$$\|u - u_{c,1}\|_{0,(0,h)} \approx \|u - u_{c,1}\|_{0,(-h,0)} \approx \sqrt{13h/48} \approx 0.5204\sqrt{h}. \quad (4.3)$$

4.2. Discontinuity non-matched mesh

In this subsection, we consider the case that the mesh is not matched with the discontinuity. From the above discussion, we notice that the size of each element is not essential (their ratio is more important, see the example below).

4.2.1. A local uniform mesh

Suppose $0 < t < 1$ and $h > 0$, we consider the following mesh with 5 elements with size h : $x_{-3} = -(t+2)h$, $x_{-2} = -(t+1)h$, $x_{-1} = -th$, $x_1 = (1-t)h$, $x_2 = (2-t)h$, and $x_3 = (3-t)h$, see the left of Fig. 3 for a test mesh with $t = 1/3$ and $h = 1$. The discontinuity cuts through the central interval $I_0 = (-th, (1-t)h)$ at 0. Let λ_i be the linear Lagrange basis function for $i = \pm 1, \pm 2, \pm 3$. As before, we assume that $u_{c,1}$ is exact at $i = \pm 3$ (we omit the small perturbation ϵ for simplicity). Then on the interval (x_{-3}, x_3) ,

$$u_{c,1} = -\lambda_{-3} + U_{-2}\lambda_{-2} + U_{-1}\lambda_{-1} + U_1\lambda_1 + U_2\lambda_2 + \lambda_3.$$

Solve the following projection problem,

$$(u_{c,1}, \lambda_i)_{(x_{-3}, x_3)} = (u, \lambda_i)_{(x_{-3}, x_3)}, \quad i = \pm 1, \pm 2,$$

we get

$$\begin{aligned} U_{-2} &= -3(87 - 60t + 38t^2)/209, & U_{-1} &= (-1 - 720t + 456t^2)/209, \\ U_1 &= (265 + 192t - 456t^2)/209, & U_2 &= 3(65 - 16t + 38t^2)/209. \end{aligned}$$

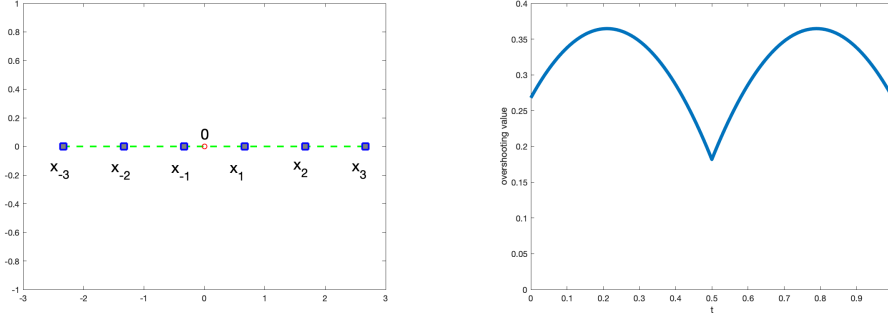
The overshooting value is defined as the following function:

$$\text{os} = \max(-(U_{-2} + 1), -(U_{-1} + 1), (U_1 - 1), (U_2 - 1), 0).$$

We plot the overshooting value with respect to t on the right of Fig.3. The overshooting values lies in the interval

$$[0.1818, 0.3646].$$

Also, we find that when $0 < t < 1/2$, the maximum overshooting happen at U_1 and when $1/2 < t < 1$, the maximum overshooting happens at U_{-1} ,



(a) a test mesh with $t = 1/3$ and $h = 1$ (b) overshooting values as $t \in (0, 1)$

Figure 3: Continuous piecewise linear approximation on a discontinuity non-aligned mesh

that is, the maximum overshooting appears at the one of the endpoints of I_0 which is farther from the discontinuity. In any choice of $0 < t < 1$, the overshooting is non-trivial.

We have the following L^2 error:

$$\|u - u_{c,1}\|_{0,I_0} = 2\sqrt{h(8869 + 60189t - 294117t^2 + 467856t^3 - 233928t^4)/131043}.$$

For $0 \leq t \leq 1$, we get $\|u - u_{c,1}\|_{0,I_0}$ is between $0.5203\sqrt{h}$ and $0.6236\sqrt{h}$. Note this error matches with the result of (4.3), which corresponds to $t = 0$ or 1 .

4.2.2. A local adaptive mesh

We also test the following mesh: $x_{-3} = -(t + 4)h$, $x_{-2} = -(t + 2)h$, $x_{-1} = -th$, $x_1 = (1 - t)h$, $x_2 = (2 - t)h$, and $x_3 = (4 - t)h$, with sizes $2h$, h , h , and $2h$, respectively. This kind mesh can be viewed as an example that the mesh is obtained by adaptive refinements.

With this mesh setting and assuming the values of $u_{c,1}$ at $x_{\pm 3}$ are exact, by a similar procedure, we get

$$\begin{aligned} U_{-2} &= 1/241(-281 + 138t - 87t^2), \\ U_{-1} &= 3/241(-27 - 184t + 116t^2), \\ U_1 &= 1/241(325 + 144t - 468t^2), \\ U_2 &= 1/241(227 - 24t + 78t^2). \end{aligned}$$

We show the result on the right of Fig.4, the overshooting value lies in the interval

$$[0.1358, 0.3954]. \tag{4.4}$$

Also, as before, we find that the maximum overshooting happens at U_1 when $0 < t < 1/2$, and it happens at U_{-1} when $1/2 < t < 1$. For any choice of $0 < t < 1$, the overshooting is non-trivial. We can vary the element size of elements adjacent I_0 from h , $2h$, $4h$, to $8h$, and get similar results of non-trivial overshootings. This shows that adaptive mesh refinements by bisection will not make the overshooting phenomena disappear for the continuous linear approximation.

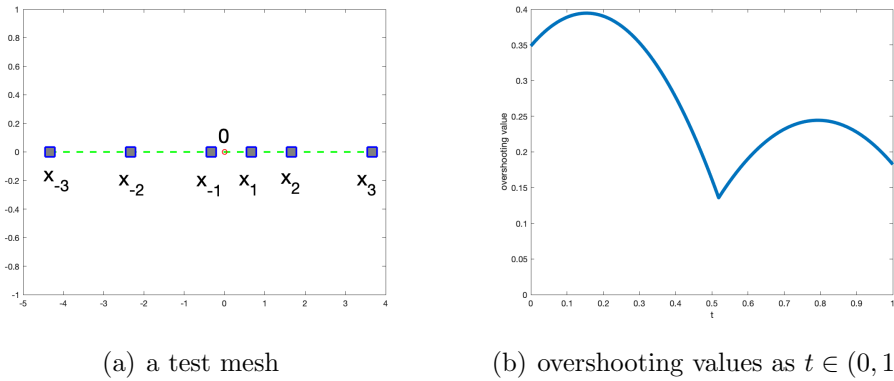


Figure 4: Continuous piecewise linear approximation on a discontinuity non-aligned non uniform mesh

We have the following L^2 error:

$$\|u - u_{c,1}\|_{0,I_0} = 2\sqrt{h(20923 + 13173t - 221541t^2 + 450576t^3 - 250668t^4)/174243}.$$

For $0 \leq t \leq 1$, we get $\|u - u_{c,1}\|_{0,I_0}$ is between $0.5349\sqrt{h}$ and $0.6965\sqrt{h}$.

4.3. Adaptive mesh with coarsening

For the one dimensional problem, there is one special case that the overshooting phenomena can be eliminated.

Consider the following mesh $\dots, x_{-2}, x_{-1}, x_0, x_1, x_2, \dots$, with $x_0 = 0$, $x_{\pm 1} = \pm h$, and $x_{\pm 2} = \pm ch$, with $h > 0$ and $c > 1$. Similar as the uniform grid case, the projection $u_{c,1}$ on (x_0, x_2) can be written as

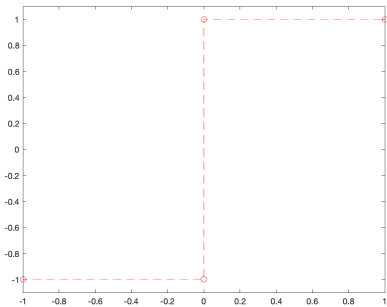
$$u_{c,1} = U_1\lambda_1 + (1 + \epsilon)\lambda_2, \quad x \in (x_0, x_2).$$

Computed by projection, we get

$$U_1 = 1 + \frac{1 - c\epsilon}{2(1 + c)}.$$

This means when the ratio $c > 1$ is big enough, the overshooting value can be reduced to a very small value. For a one dimensional mesh, this is possible by combining the refining and coarsening, i.e., when an a posteriori error indicator on an element K is big, then element is refined, while for those elements with small indicators, they are combined with the close elements to form bigger elements.

We test the case with the following example: the domain is $(-1, 1)$, the initial mesh is $[-1; -1/3; 2/3; 1]$. We use the exact L^2 error as the error estimator, i.e., $\eta_K = \|u - u_{c,1}\|_{0,K}$, and set the refinement/coarsening criteria as "refine those elements whose $\eta_K > 0.6 \max_{\{T \in \mathcal{T}_h\}} \eta_T$ and coarsen those elements whose $\eta_K < 0.3 \max_{\{T \in \mathcal{T}_h\}} \eta_T$ ". For this very simple problem, the final mesh will only contains three elements, a center very small element around 0, and two big elements on the left and right, receptively. After 14 iterations, the final mesh is $[-1; -0.0000814; 0.0000407; 1]$, and the numerical solution at four nodes are $[-1; -1.00008; 0.99998; 1.0]$. The overshooting phenomena is almost invisible.



(a) overshooting values as $t \in (0, 1)$

Figure 5: Continuous piecewise linear approximation with adaptive refinement/coarsening

Note that such case will only happen in one dimensional setting. In two and three dimensions, if we have to keep the mesh conforming and regular, the ratio of mesh sizes between two adjacent elements sharing a same edge/face cannot be big, thus there will always be non-trivial overshootings. Even for one dimensional problems, such high ratio mesh is probably not possible due to other approximation errors to keep the mesh from coarsening, see a numerical test in Section 5.

5. Numerical Test 1: a 1D singularly perturbed problem

Consider the following problem:

$$-\epsilon u'' + u = f, \quad \text{on } (0, 1), \quad \text{and} \quad u(0) = u(1) = 0, \quad (5.5)$$

where

$$f = \begin{cases} 2x & x < 1/2, \\ 2x - 2 & x > 1/2. \end{cases}$$

We choose $\epsilon = 10^{-16}$. For ϵ this small, the solution is almost identical to f , and has an extremely sharp layer at $x = 1/2$. For the case that mesh size is not small enough to match with the layer, $x = 1/2$ can be viewed as a discontinuity location.

We test the problem with three numerical methods: the linear C^0 -conforming finite element method, linear discontinuous Galerkin finite element method, and the lowest-order mixed method.

Let $0 = x_0 < x_1 < \dots < x_N = 1$ be a one-dimensional mesh \mathcal{T}_h of $(0, 1)$, with $K_i = (x_i, x_{i+1})$ and $h_i = x_{i+1} - x_i$.

Linear conforming finite element method (P1 conforming): Find $u_h \in S_{1,0}(\mathcal{T}_h)$, such that

$$(\epsilon u_h', v') + (u_h, v) = (f, v), \quad v \in S_{1,0}(\mathcal{T}_h). \quad (5.6)$$

where $S_{1,0}(\mathcal{T}_h) = S_1(\mathcal{T}_h) \cap H_0^1(\Omega)$. Note that for a very small ϵ , this is the L^2 -projection to $S_{1,0}(\mathcal{T}_h)$ we discussed.

Linear discontinuous Galerkin finite element problem (P1-DG): Find $u_{dg} \in P_1(\mathcal{T}_h)$, such that

$$a_{dg}(u_{dg}, v) = (f, v), \quad \forall v \in P_1(\mathcal{T}_h), \quad (5.7)$$

where

$$\begin{aligned} a_{dg}(w, v) &:= (\epsilon w', v')_{\mathcal{T}_h} + (w, v)_{\mathcal{T}_h} - \sum_{i=1}^{N-1} (\{\epsilon w'(x_i)\} \llbracket v(x_i) \rrbracket + \{\epsilon v'(x_i)\} \llbracket w(x_i) \rrbracket) \\ &\quad + \sum_{i=1}^{N-1} \frac{\epsilon \mu}{h_i + h_{i-1}} \llbracket w(x_i) \rrbracket \llbracket v(x_i) \rrbracket, \end{aligned}$$

where $\mu > 0$ is a big enough number (we can safely choose $\mu = 10$). This is the L^2 -projection to $P_1(\mathcal{T}_h)$ for a very small ϵ .

To introduce the mixed method, we let $\sigma = -\epsilon u' \in H^1(0, 1)$, then $\sigma' + u = f$. The mixed variational formulation is: find $(\sigma, u) \in H^1(0, 1) \times L^2(0, 1)$, s.t.,

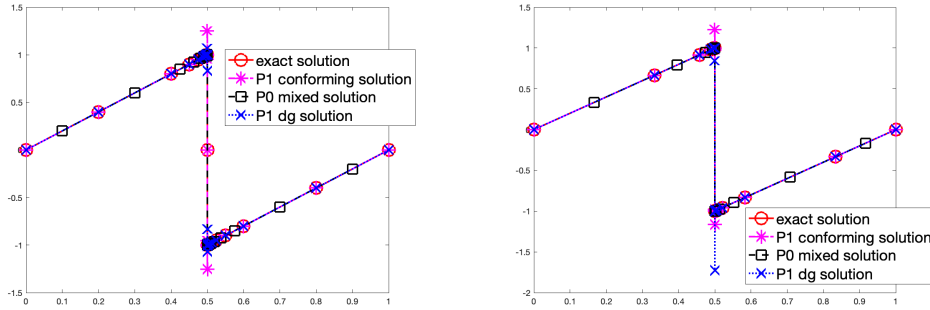
$$\begin{cases} (\epsilon^{-1}\sigma, \tau) - (\tau', u) = 0, & \forall \tau \in H^1(0, 1), \\ -(\sigma', v) - (u, v) = -(f, v), & \forall v \in L^2(0, 1). \end{cases} \quad (5.8)$$

We choose the approximation spaces to be S_1 and P_0 for σ and u , respectively. **Mixed finite element problem (P0 mixed):** Find $(\sigma_h, u_h) \in S_1(\mathcal{T}_h) \times P_0(\mathcal{T}_h)$, s.t.,

$$\begin{cases} (\epsilon^{-1}\sigma_h, \tau) - (\tau', u_h) = 0, & \forall \tau \in S_1(\mathcal{T}_h), \\ -(\sigma_h', v) - (u_h, v) = -(f, v), & \forall v \in P_0(\mathcal{T}_h). \end{cases} \quad (5.9)$$

This is the L^2 -projection to $P_0(\mathcal{T}_h)$ for a very small ϵ .

In the computation, we use the robust error estimator for the conforming finite element method in [14, 9] to drive the adaptive mesh refinement and compute the conforming, DG, and mixed finite element solutions on the same adaptive mesh.



(a) solutions with a discontinuity on a mesh matched at the discontinuity (b) solutions with a discontinuity on a non-matched mesh

Figure 6: 1D reaction-diffusion problem with adaptive refinement on discontinuity matched and non-matched meshes

Discontinuity matched mesh case. An initial mesh $[0; 0.2; 0.4; 0.6; 0.8; 1]$ is chosen. We refine it for 20 times with the maximum refinement strategy $\theta = 0.8$. The center nodes are $0.5 + 10^{-6} \times [-0.3815; -0.1907; 0; 0.1907; 0.3815]$. Numerical approximations with linear conforming, P0-mixed, and P1-DG approximations are shown in Fig. 6. The overshooting value for the linear conforming finite element approximation is $1.2546 - 1 = 0.2546$, which matches

discontinuity matched case. The P0-mixed solution has no overshooting due to that it is a piecewise constant approximation, and the P1-DGFEM has no overshooting since the discontinuity is matched with the mesh.

Discontinuity non-matched mesh case. Next, we choose an initial mesh $[0; 1/3; 5/6; 1]$. With bisections, the discontinuity location will never be exactly matched. The center nodes are $0.5 + 10^{-5} \times [-0.2543; -0.0636; -0.0159; 0.0318; 0.1272; 0.5086]$. The values of linear conforming solution u_h at two nodes adjacent to $1/2$ are 1.2284 and -1.1647 . This also matches the discussion in (4.4). A value of -1.7242 is found of P1-DGFEM approximation at the node $x = 0.0318$. The value is a little big larger than the discussion in Section 3.2, where piecewise linear function is used to approximate a discontinuous step function, while here it is a discontinuous piecewise linear function. The discontinuous mixed solution has no overshooting for this case.

For a similar problem, in the bottom page 165 of [4], the authors claimed that the DG method for this problem will have no oscillations. This is incorrect, the DG method will have no oscillations unless the discontinuity is matched with the mesh. The numerical test in [4] uses a uniform mesh with $h = 1/N$, which is exactly the discontinuity matched case. Thus, the non-overshooting in [4] is not only due to the use of DGFEM, but because of using DGFEM on a discontinuity-matched mesh.

Adaptive mesh with both refinement and coarsening. Next we test the problem with both refine and coarsening. The initial mesh is chosen to be a uniform mesh with $h = 1/17$, and the nodes on the final mesh are $0, 0.4926, 0.4926, 0.9412, 1.0000$. The C^0 conforming finite element solution u_h at these nodes are $0, 0.95, -1.05, -0.10, 0$ with almost no overshooting, see Fig. 7.

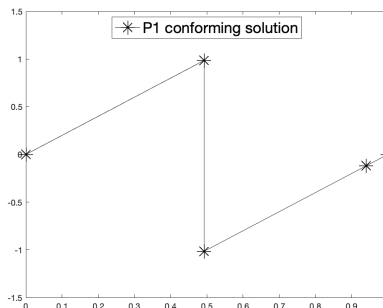


Figure 7: One-D reaction-diffusion problem with adaptive refinement/coarsening

We should point out that it is not always possible to get a high ratio mesh such as that in of Fig. 7 with a combination of an adaptive refinement and coarsening. We test the problem with the righthand side:

$$f_2 = \begin{cases} x^2 & x < 1/2, \\ x^2 - 1 & x > 1/2. \end{cases}$$

Note that for the linear finite element approximation, there is some approximation error on all elements. Thus these elements are not coarsened, we eventually have a standard adaptively refined mesh and overshooting phenomena appears, see Fig. 8.

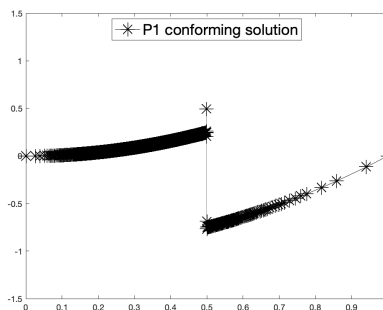


Figure 8: One-D reaction-diffusion problem, adaptive refinement and coarsening with f_2

6. Numerical Test 2: DG methods for a linear transport equation in 2D

Consider the following linear transport (advection) equation:

$$\begin{aligned} \nabla \cdot (\boldsymbol{\beta}u) + \gamma u &= f \quad \text{in } \Omega, \\ u &= g \quad \text{on } \Gamma_-, \end{aligned} \tag{6.10}$$

where the advective velocity field $\boldsymbol{\beta} = (\beta_1, \beta_2)^T \in [C^1(\bar{\Omega})]^2$ is a vector-valued function defined on $\bar{\Omega}$ and $\gamma \in L^\infty(\Omega)$. The inflow part of $\partial\Omega$, $\Gamma_- = \{x \in \partial\Omega : \boldsymbol{\beta}(x) \cdot \mathbf{n}(x) < 0\}$, is defined in the usual fashion, where $\mathbf{n}(x)$ denotes the unit outward normal vector to $\partial\Omega$ at $x \in \partial\Omega$.

The DGFEM for the transport equation is [2]: find $u_h \in P_k$, $k = 0$ or 1 such that

$$a_{dg}(u_h, v_h) = f(v_h), \quad \forall v_h \in P_k, \tag{6.11}$$

where the bilinear form and linear form are defined by

$$a_{dg}(w_h, v_h) := \sum_{K \in \mathcal{T}_h} (w_h, -\boldsymbol{\beta} \cdot \nabla v_h + \gamma v_h)_K + \sum_{F \in \mathcal{E}_I \cup \mathcal{E}_{out}} (\{\boldsymbol{\beta} \cdot \mathbf{n} w_h\}_{up}, \llbracket v_h \rrbracket)_F,$$

$$f(v_h) = (f, v_h) - \sum_{F \in \mathcal{E}_{in}} (\boldsymbol{\beta} \cdot \mathbf{n} g, v_h)_F,$$

where the term $\{\boldsymbol{\beta} \cdot \mathbf{n} w_h\}_{up}$ is the usual upwind flux, meaning that $\{\boldsymbol{\beta} \cdot \mathbf{n} w_h\}_{up}$ takes the value on the inflow side of the edge/face F . The sets \mathcal{E}_{in} , \mathcal{E}_I , and \mathcal{E}_{out} are the sets of inflow, interior, and outflow edges, respectively. We call the methods P0-DGFEM and P1-DGFEM for $k = 0$ and 1, respectively.

We use a residual type of error estimator similar to that developed in [3] to drive the adaptive mesh refinement.

6.1. A discontinuous solution on a non-matching mesh

Consider the problem: $\Omega = (0, 2) \times (0, 1)$ with $\boldsymbol{\beta} = (0, 1)^T$. The inflow boundary is $\{x \in (0, 1), y = 0\}$. Let $\gamma = 0$ and $f = 0$. Choose the inflow boundary condition such that the exact solution is

$$u(x, y) = \begin{cases} 0 & \text{if } x < \pi/3, \\ 1 & \text{if } x > \pi/3. \end{cases}$$

The initial mesh is shown on the left of Fig. 9. The point $(\pi/3, 0)$ and $(1, 1)$ are the bottom central node and the top central node, respectively. The mesh and its subsequent bisection mesh are not aligned with the discontinuity although the inflow boundary condition is matched.

On the center of Fig. 9, a final adaptive mesh is shown with many refinements along the discontinuity since the mesh is not matched. On the right of Fig. 9, we show the overshooting values of the P1-DGFEM, with the overshooting value defined as:

$$\text{os} = \max\{u_h - 1, -(u_h + 1), 0\}.$$

From the figure, we see that the overshooting values are oscillate between 0.15 and 0.35 and never goes to zero, which is matched with our analysis. For the P0-DGFEM, the overshooting value is in the order of machine accuracy, 10^{-16} , so there is no overshooting at all.

Since the exact solution of the problem is not changing with respect to the y -coordinate, we plot a projected solution by plotting the numerical solutions the element center (P_0)/ nodes (P_1) suppressing the y -coordinate. On

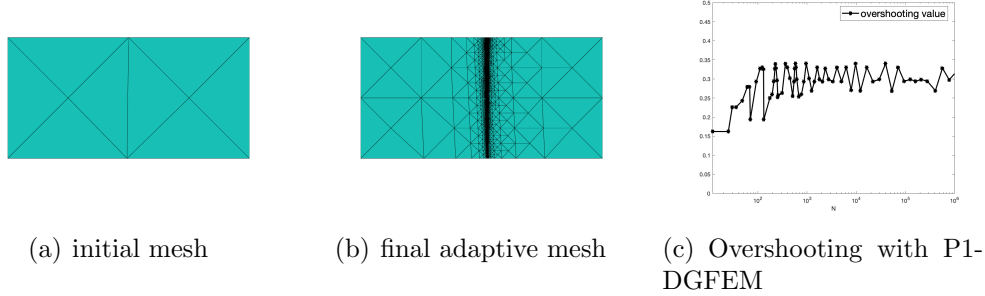


Figure 9: Piecewise constant solution transport problem with a non-matching grid test problem

Fig. 10, we show the P0-DGFEM projected solution computed on the final adaptive mesh on the left and P1-DGFEM one on the right. We clear see the overshooting of P1-DGFEM.

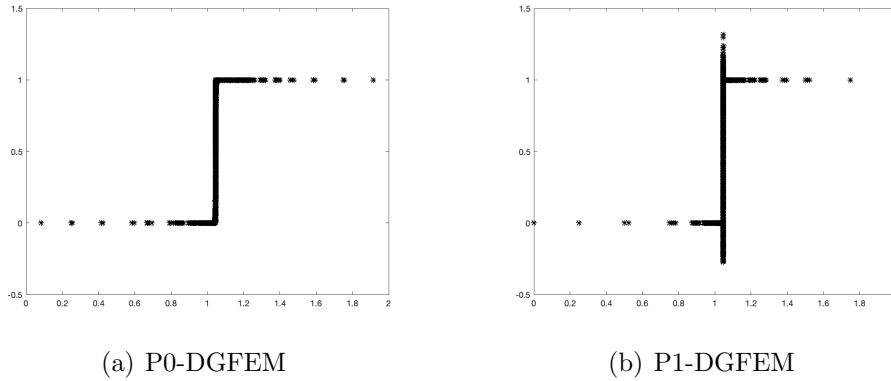


Figure 10: Projected solutions with P0- and P1-DGFEMs for piecewise constant solution transport problem on a non-matching mesh

6.2. Curved transport problem 1

Consider the problem on the half disk $\Omega = \{(x, y) : x^2 + y^2 < 1; y > 0\}$. The inflow boundary is $\{-1 < x < 0; y = 0\}$. Let $\beta = (\sin \theta, -\cos \theta)^T = (y/\sqrt{x^2 + y^2}, -x/\sqrt{x^2 + y^2})^T$, with θ is the polar angle. Let $\gamma = 0$, $f = 0$, and the inflow condition and the exact solution be

$$g = \begin{cases} 1 & \text{if } -1 < x < -0.5, \\ 0 & \text{if } -0.5 < x < 0, \end{cases} \quad \text{and} \quad u = \begin{cases} 1 & \text{if } x^2 + y^2 > 0.25, \\ 0 & \text{otherwise.} \end{cases}$$

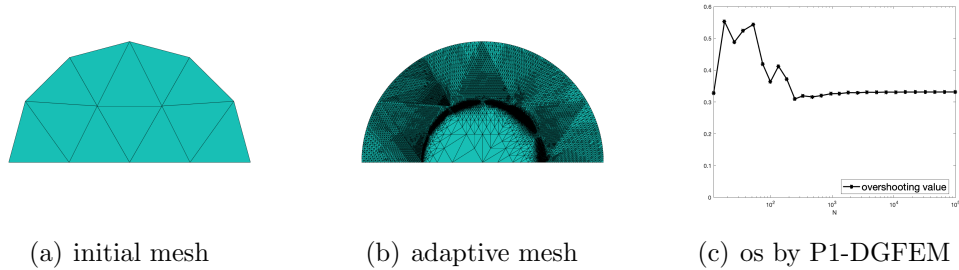


Figure 11: P1-DGFEMs for the curved transport problem 1

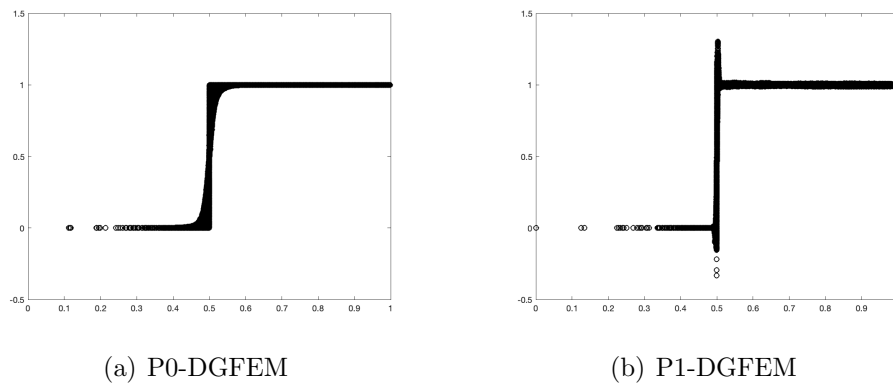


Figure 12: Projected solutions with P0 and P1-DGFEMs for curved transport problem 1

The initial mesh is shown on the left of Fig. 11. On the center of Fig. 11, a final adaptive mesh is shown. On the right of Fig. 9, we show the overshooting values of the P1-DGFEM, with the overshooting value defined as:

$$\text{os} = \max\{u_h - 1, -u_h, 0\}.$$

From the figure, we see that the overshooting values are oscillate between 0.3 and 0.6 and never goes to zero with the mesh refinements.

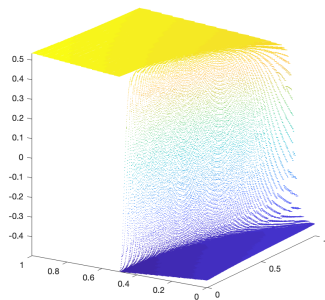
We plot projected solutions by plotting the numerical solutions the element center (P_0)/ nodes (P_1) with respect to the radius on Fig. 12, we show the P0-DGFEM projected solution computed on the final adaptive mesh on the left and the P1-DGFEM one on the right. We clearly see the overshooting of P1-DG approximation but non-overshooting of the P0-DG approximation.

6.3. Curved transport problem 2

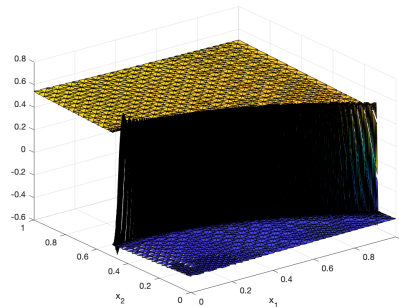
Consider the following problem: $\Omega = (0, 1)^2$ with $\boldsymbol{\beta} = (y+1, -x)^T / \sqrt{x^2 + (y+1)^2}$, $\gamma = 0.1$, and $f = 0$. The inflow boundary is $\{x = 1, y \in (0, 1)\} \cup \{x \in (0, 1), y = 0\}$, i.e., the west and north boundaries of the domain. Choose g such that the exact solution u is

$$u = \frac{1}{4} \exp\left(\gamma r \arcsin\left(\frac{y+1}{r}\right)\right) \arctan\left(\frac{r-1.5}{\epsilon}\right), \quad \text{with } r = \sqrt{x^2 + (y+1)^2}.$$

When $\epsilon = 10^{-10}$, the layer is never fully resolved in our experiments and can be viewed as discontinuous. In Fig. 13, we show numerical solutions by P0- and P1-DGFEMs. It is easy to see that there is no overshooting for the P0-DGFEM solution, and non-trivial overshooting can be found for the P1-DGFEM solution.



(a) P0-DGFEM



(b) P1-DGFEM

Figure 13: Numerical solutions with adaptive P0- and P1-DGFEMs for Curved Transport Problem 2

Similar results are available for these three numerical tests with $H(\text{div})$ flux based least-squares finite element formulations can be found in [11].

7. Concluding Remarks

In this paper, we studied the behavior of using adaptive continuous and discontinuous finite elements to approximate discontinuous and nearly discontinuous PDE solutions.

For a singularly perturbed problem with a small diffusion or other equations with a transient layer, when the mesh is fine enough around the transient layer, the numerical solution can accurately approximate the PDE solution. This is the case that the belief that the adaptive finite element works come from.

For a pre-asymptotic mesh of such layer problems, the solution can be viewed as discontinuous and we can treat it identically as the genuinely discontinuous case.

To approximate a discontinuous solution, the global continuous function is always a bad choice since it will always have non-trivial oscillations. Other than that, it will hard to impose a discontinuous boundary boundary condition with a continuous approximation space. If the exact location of the discontinuity is known, then high order discontinuous approximations on a discontinuity-matched mesh is a good choice. For singularly perturbed problems with a small diffusion, this mesh-matched case is reduced to that the mesh interface lies within the small transient layer. If the location of the discontinuity is unknown, the only way to avoid the overshooting is to use piecewise constant approximations for those elements where a discontinuity cuts through. Discontinuous piecewise linear function approximations will have non-trivial overshooting for most cases. The adaptive finite element method with a good a posteriori error estimator can reduce the L^2 -norms (or H^1 and other integration based norms) of the error, but it cannot reduce the non-trivial oscillations unless a piecewise constant approximation is used in the discontinuity-crossing elements.

The non-trivial overshooting we find in the paper is of the same magnitude as the Gibbs phenomena in the Fourier analysis, where a number around 0.17 of the jump gap is found, see [8].

With the above results in mind, when we design finite element methods for problems with unknown location discontinuous solutions, an hp adaptivity approach is preferred. We use high order finite elements (continuous or discontinuous) in the smooth region and use piecewise constant approximations in the discontinuity-crossing elements. This is one of our ongoing work. It is also worth to mention that the method proposed by Lax [10] is exactly such a method in the context of the finite difference method.

References

- [1] M. J. BERGER AND J. OLIGER, *Adaptive mesh refinement for hyper-*

hyperbolic partial differential equations, Journal of Computational Physics, Volume 53, Issue 3, March 1984, Pages 484–512.

- [2] F. BREZZI, L. D. MARINI, AND E. SÜLI, *Discontinuous galerkin methods for first-order hyperbolic problems*, Mathematical Models and Methods in Applied Sciences, 14 (2004), pp. 1893–1903.
- [3] E. BURMAN, *A posteriori error estimation for interior penalty finite element approximations of the advection-reaction equation*, SIAM J. Numer. Anal., Vol. 47, No. 5, pp. 3584–3607.
- [4] S. FRANZ AND H-G. ROOS, *The capriciousness of numerical methods for singular perturbations*, SIAM Review, Vol. 53, No. 1 (2011), pp. 157–173.
- [5] D. GOTTLIEB AND C.-W. SHU, *The Gibbs phenomenon and its resolution*, SIAM Review, 39 644-668, 1997.
- [6] J. S. HESTHAVEN, *Numerical Methods for Conservation Laws: From Analysis to Algorithms*, SIAM, 2018.
- [7] J. S. HESTHAVEN AND T. WARBURTON, *Nodal Discontinuous Galerkin Methods: Algorithms, Analysis, and Applications*, Texts in Applied Mathematics (TAM), vol. 54, Springer, 2008.
- [8] E. HEWITT AND R. HEWITT, *The Gibbs-Wilbraham phenomenon: An episode in Fourier analysis*, Archive for History of Exact Sciences. 21 (2): 129–160, 1979.
- [9] G. KUNERT, *A note on the energy norm for a singularly perturbed model problem*, Computing, vol 69, 3, 2002, 265–272.
- [10] P. D. LAX, *Gibbs phenomena*, J. Sci. Computing, 28(2-3):445–449, 2006.
- [11] Q. LIU AND S. ZHANG, *Adaptive least-squares finite element methods for linear transport equations based on an $H(\text{div})$ flux reformulation*, arxiv 1807.01524, 2018.
- [12] H.-G. ROOS, M. STYNES, AND L. TOBISKA, *Robust Numerical Methods for Singularly Perturbed Differential Equations*, Springer Ser. Comput. Math., Springer, Berlin, Heidelberg, 2008.

- [13] C.-W. SHU, *Essentially non-oscillatory and weighted essentially non-oscillatory schemes for hyperbolic conservation laws*, in *Advanced Numerical Approximation of Nonlinear Hyperbolic Equations*, B. Cockburn, C. Johnson, C.-W. Shu, E. Tadmor, and A. Quarteroni, eds., *Lecture Notes in Math.* 1697, Springer-Verlag, Berlin, 1998, pp. 325–432.
- [14] R. VERFÜRTH, *Robust a posteriori error estimators for a singularly perturbed reaction-diffusion equation*, *Numer. Math.* (1998) 78, 479–493.
- [15] R. VERFÜRTH, *A Posteriori Error Estimation Techniques for Finite Element Methods*, Oxford University Press, Oxford, UK, 2013